

STRUCTURAL CAPACITY EVALUATION OF DRILLED SHAFT  
FOUNDATIONS WITH DEFECTS

by

Khamis Y. Haramy  
B.S. Virginia Tech, 1979

A thesis submitted to the  
University of Colorado at Denver  
in partial fulfillment  
of the requirements for the degree of  
Master of Science  
Civil Engineering  
2006

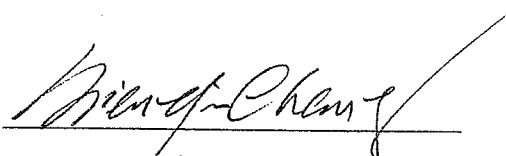
This thesis for the Master of Science

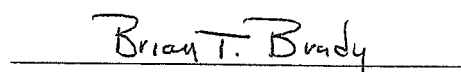
degree by


Khamis Y. Haramy

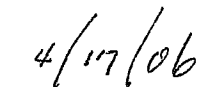
has been approved

by

  
Dr. Nien Yin Chang

  
Dr. Brian T. Brady

  
Dr. Aziz Khan

  
Date

Haramy, Khamis Y. (M.S. Civil Engineering)  
Structural Capacity Evaluation of Drilled Shaft Foundations with Defects  
Thesis directed by Professor Nien Yin Chang

## **ABSTRACT**

Drilled shafts have become very popular deep foundation supports. Drilled shafts can be constructed in a wider range of ground conditions with less noise and vibration than driven piles. Quality assurance (QA) and quality control (QC) of drilled shafts has become a concern due to difficulties in locating defects and determining load bearing capacity. Various non-destructive evaluation (NDE) techniques have been developed to estimate the integrity of the concrete. While NDE techniques provide a powerful tool and have been widely accepted, many variables and unknowns can affect the measurement results. Results are more difficult to interpret, leading to unnecessary litigation over shaft integrity. In addition, influences of surrounding ground, stress states under different load conditions, and crack development during concrete curing further complicate determination of shaft performance.

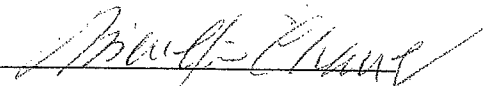
This study focuses on the load bearing capacity evaluation of drilled shafts under various conditions by analysis methods and numerical models. The analysis is approached first from identification of design criterion and construction procedures, with a brief review of NDE techniques. The analysis method is based on principles and theorems from engineering mechanics, geotechnical engineering, concrete chemistry, and geophysical engineering. The analysis results are used as input to the numerical analysis. The numerical model employed in this research is incorporated into the Geostructural Analysis Package (GAP), combining the widely accepted numerical methods of Discrete Element Method (DEM), Particle Flow Method (PFM), Material Point Method (MPM), and Finite Differencing (FD), together with engineering mechanics constitutive models, concrete chemistry models,

thermodynamics models, and geophysical tomography and holography for geotechnical engineering application. GAP has been successfully used for ground characterization in highway engineering and mining operations.

This study explores many concerns recently raised for drilled shaft design, construction and maintenance. Recommendations and conclusions may provide engineers with more information and a better understanding of drilled shaft foundations to revolutionize foundation design, concrete mix design, construction techniques, NDE measurement, and defect evaluation, to improve performance and efficiency with reduced litigation risk.

This abstract accurately represents the content of the candidate's thesis. I recommend its publication.

Signed



Dr. Nien Yin Chang

## DEDICATION

I dedicate this thesis to my wife, Kathy Haramy, and my supervisor, Bob Welch, for their unfaltering understanding and support while I was pursuing my master's degree and writing this thesis.

## ACKNOWLEDGMENT

I would like to acknowledge several persons who contributed to the completion of this thesis. This research could not have been possible without the support and funds from Mr. Roger Surdahl, the Technology Development Coordinator at the FHWA-CFLHD, Mr. Alan Rock, Dr. Runing Zhang, and Dr. David Wilkinson for developing the modeling programs that were used for the analysis. I would also like to thank Mr. Frank Jalinoos and Ms. Natasa Mekic-Stall for their assistance in data collection. I would also like to acknowledge the efforts of all the committee members for their contributions, including Dr. Nien Yin Chang, Dr. Brian Brady, and Dr. Aziz Khan.

## CONTENTS

Figures.....	xiii
Tables.....	xxiii
<u>Chapter</u>	
1 Introduction.....	1
1.1 Purpose and Objectives.....	5
1.2 Background-Drilled Shaft Foundations .....	7
1.2.1 Description.....	7
1.2.2 Advantages and Disadvantages.....	12
1.2.3 Construction Inspection and Observation Methods.....	13
1.2.3.1 Down-Hole Inspections .....	14
1.2.3.2 Probe Inspection.....	14
1.2.3.3 Video Camera Inspection.....	15
1.2.3.4 Shaft Wall Sampling and Rock Socket Wall Roughness Inspection.....	16
1.2.3.5 Electro-Mechanical and Acoustic Shaft Caliper.....	17
1.3 NDE Methods for Determining Drilled Shaft Integrity .....	18
1.3.1 Overview.....	19
1.3.1.1 History of Non-Destructive Evaluation Methods .....	19
1.3.1.2 Summary of a National DOT Synthesis on Use of NDE Methods.....	22
1.3.2 Sonic Echo and Impulse Response (SE and IR) .....	25
1.3.2.1 Basic Theory and Procedures.....	27
1.3.2.2 Applications/Limitations.....	29
1.3.2.3 Testing Equipment.....	32
1.3.2.4 Defect Definition .....	32
1.3.3 Gamma-Gamma Density Logging (GDL).....	32
1.3.3.1 Basic Theory and Procedures.....	32

1.3.3.2 Applications/Limitations.....	33
1.3.3.3 Testing Equipment.....	34
1.3.3.4 Defect Definition .....	34
1.3.4 Crosshole Sonic Logging (CSL).....	37
1.3.4.1 CSL Basic Theory.....	37
1.3.4.2 CSL Applications/Limitations .....	43
1.3.4.3 CSL Testing Equipment.....	44
1.3.4.4 CSL Test Procedures and Results.....	53
1.3.5 Other Specialized Logging Methods .....	57
1.3.5.1 Neutron Moisture Logging (NML).....	57
1.3.5.2 Temperature Logging.....	58
2 CSL Data Processing and Interpretation Using 3-D Tomography .....	60
2.1 Basic Principles for 3-D Tomography .....	60
2.2 Case Studies.....	63
2.2.1 Bridge Foundation Construction Site 1.....	64
2.2.1.1 CSL Test Procedures.....	66
2.2.1.2 CSL Test Results and Analysis.....	71
2.2.1.3 Tomographic Imaging of the CSL Test Results .....	73
2.2.2 Bridge Foundation Construction Site 2.....	74
2.2.2.1 CSL Test Procedures.....	78
2.2.2.2 CSL Test Results and Analysis.....	83
2.2.2.3 Tomographic Imaging of the CSL Test Results .....	85
2.2.2.4 Pile Repair Procedure .....	91
2.3 Tomographic Imaging Summary and Recommendations.....	99
3 Field Monitoring of Drilled Shaft Temperature, Velocity, Density, and Moisture	101
3.1 Temperature Monitoring.....	101
3.1.1 Temperature Logging in Drilled Shaft 1 Abutment 1.....	102
3.1.2 Temperature Logging in Drilled Shaft 2-Pier 2.....	106
3.1.3 Temperature Monitoring With Thermocouples .....	109

3.1.4 Temperature Monitoring - Conclusion .....	111
3.2 Velocity Monitoring Results.....	112
3.3 Density Monitoring.....	115
3.4 Moisture Monitoring.....	123
3.5 Summary of NDE Monitoring .....	125
4 Concrete Defects and Curing Chemistry .....	128
4.1 Hydration Rates and Heat Generation during Concrete Curing .....	130
4.2 Curing Chemistry Modeling .....	133
4.2.1 Empirical Modeling Methods .....	134
4.2.2 Micro-Modeling Methods (M3).....	135
4.3 Thermal Issues for Concrete Construction in the Field .....	136
4.3.1 General Aspects of Thermal Cracking Analyses .....	137
4.3.2 Problems with the 20 °C Limit.....	139
4.3.3 The Importance of Thermal Modeling in Concrete Structural Design and NDE .....	140
4.4 Engineering Practice for Controlling Thermal Issues in Concrete Construction	141
4.4.1 Temperature Profiling.....	141
4.4.2 Simple and Practical Techniques for Reducing Thermal Concrete Cracking With Standard Construction Techniques .....	142
4.4.2.1 Concrete Placement Temperature .....	142
4.4.2.2 Aggregate Properties.....	143
4.4.2.3 Cement Properties.....	143
4.4.3 Field Measures to Reduce $\Delta T$ , Techniques and Implications .....	145
4.4.3.1 Special Construction Measures.....	145
4.5 Comparative Evaluation of Thermal Control Measures .....	146
4.6 Environmental Effects on Curing Chemistry and Concrete Quality .....	148
4.6.1 Changes in Ground Water Heat Conductivity .....	150
5 Numerical Modeling .....	152
5.1 Establishment of Numerical Model .....	153
5.2 Theoretical Models .....	154

5.3 Thermal Modeling .....	155
5.4 Engineering Mechanics.....	161
5.5 Discrete Element Method (DEM) Background .....	165
5.5.1 Discrete Element Method Definition .....	167
5.5.2 Equation of Motion.....	168
5.5.3 Contact Mechanics.....	171
5.5.3.1 Non-Linear Hertz-Mindlin Contact Model.....	172
5.5.3.2 The Visco-Elastic Contact Model.....	176
5.5.4 Validation of Numerical Models .....	179
5.5.4.1 Energy Conservation.....	179
5.5.4.2 Damping and Dynamic Relaxation (DR) Tests .....	181
5.5.4.3 Wave Propagation.....	183
6 Numerical Modeling Analysis of CSL in Drilled Shafts .....	186
6.1 Geostuctural Analysis Package (GAP) Model Description.....	186
6.2 Factors Affecting CSL Velocity Measurements .....	190
6.3 CSL Velocity Variations.....	195
6.4 Effect of Surrounding Material on CSL Signals.....	195
6.5 CSL Wave Interaction with Rebar .....	204
6.6 Tube Effects .....	212
6.6.1 Tube Material: PVC versus Steel Tubes.....	214
6.6.2 Tube Debonding.....	222
6.6.3 Sensor Drift within the Access Tubes.....	231
6.7 Concrete Cracking Effects .....	238
6.7.1 Concrete Strength Reduction .....	246
6.8 Honeycombs Effects .....	247
6.9 Effect of Voids.....	255
7 Numerical Modeling of Concrete Curing .....	263
7.1 Empirical Curing Model Method.....	263
7.2 Curing Model Presentation .....	266

7.3 Curing Model Simulation .....	268
7.3.1 Compression .....	269
7.3.2 Cracking .....	276
7.3.3 Heat .....	282
7.3.4 Hydration .....	286
7.3.5 Temperature .....	286
7.4 Discussion .....	296
8 Numerical Testing of Axial Load Capacity of a Drilled Shaft with Anomalies....	299
8.1 Axial Loading Model Analysis .....	299
8.1.1 Displacement of 4 mm .....	301
8.1.2 Displacement of 4 cm .....	304
8.1.3 Displacement of 8 cm .....	307
8.1.4 Displacement of 12 cm .....	310
8.1.5 Displacement of 16 cm and 20 cm .....	313
8.2 Load-Settlement Curve Analysis .....	313
8.2.1 Loosened Soil .....	318
8.3 Discussion .....	320
9 Summary, Conclusions, and Recommendations for Future Research .....	323
9.1 Use and Interpretation of CSL Data .....	323
9.1.1 Effects of CSL Access Tubes .....	323
9.1.2 The Potential of Numerical Modeling .....	324
9.1.3 Concrete Curing and Stress .....	325
9.2 Suggestions for Improvements .....	325
9.2.1 Use and Interpretation of CSL Data .....	325
9.2.2 Use of CSL Access Tubes .....	325
9.2.3 Concrete Pouring .....	325
9.3 Suggestions for Future Direction .....	326

<u>Appendix A</u> .....	327
<u>Appendix B</u> .....	337
<u>Appendix C</u> .....	341
<u>References</u> .....	361

## FIGURES

Figure 1.1 Photo. 3m Diameter, 32m Deep Drilled Shaft Foundation for a Bridge Structure Located at State Highway 19 over the Missouri River at Vermillion, South Dakota.....	2
Figure 1.2 Schematic Diagram of a Typical Drilled Shaft Foundation. ....	9
Figure 1.3 Photo Showing Drilled Shaft Construction .....	10
Figure 1.4 A Schematic Showing the CSL Setup .....	21
Figure 1.5 State DOT Survey Participants.....	23
Figure 1.6 Map Showing the Responding State DOTs that Use NDE for QA/QC of Drilled Shafts .....	23
Figure 1.7 The Survey Results for the Question; “Does your state DOT use NDE for QA/QC of drilled shafts?” .....	24
Figure 1.8 Survey Results for the Questions a) Which is the primary NDE method your state uses for drilled shafts and b) What is the main reason your state selects the primary NDE method? .....	26
Figure 1.9 Sonic Echo and Impulse Response Equipment and Setup. ....	28
Figure 1.10 Sonic Echo Record and Depth Calculation .....	30
Figure 1.11 Depth Calculations Using Frequency Domain Data for the Impulse Response Method.....	31
Figure 1.12 Gamma-Gamma Density Logging Equipment. (AMEC Earth & Environmental, Inc.) .....	35
Figure 1.13 Gamma-Gamma Density Logs and Results. (Geophysics, 2002) .....	36
Figure 1.14 Basic Wave Elements .....	39
Figure 1.15 Freedom NDTPC Family of Instruments (Olson Engineering, Inc.) .....	47
Figure 1.16 PILELOGs – Full Waveform Cross-hole Sonic Logging System (InfraSeis, Inc.) .....	50
Figure 1.17 PISA – Pile Integrity Sonic Analyzer (Geosciences Testing and Research, Inc.) .....	52
Figure 1.18 (a) Full Waveform Stacked Traces (InfraSeis, Inc.) and (b) CSL Log Plot –First Arrival Time (FAT), Apparent Velocity and Relative Energy Versus Depth (GRL & Assoc., Inc.) .....	55
Figure 1.19 Drilled Shaft with Defects .....	56

Figure 2.1 Pictures Showing Locations of (a) Boring B-5, (b) Boring B-6, and (c) Boring B-7 .....	65
Figure 2.2 Schematic of Site 1 Bridge Plan and Subsurface Profile .....	67
Figure 2.3 Drilled Shaft, (a) Horizontal Cross-Section, (b) Vertical Cross-Section .	68
Figure 2.4 Drilled Shaft Installation and CSL Measurements .....	70
Figure 2.5 3-D and 2-D Tomographic Representations of the A1-S2 Shaft Interior. Green Represents Velocity Contours of “Questionable” Zones .....	75
Figure 2.6 Schematic of Site 2 Bridge Plan and Subsurface Profile .....	77
Figure 2.7 Drilled Shaft Details (a) Horizontal Cross-Section, (b) Vertical Cross-Section.....	79
Figure 2.8 Variations in Apparent Velocity Due to Non-Uniform Tube Spacing. CSL Log from CP4 between Tubes 2&3 .....	83
Figure 2.9 (a) Initial CLS Test of the A2-4, (b) CSL Test of the A2-4 After 16 Days of Curing .....	86
Figure 2.10 Difference Tomograms Between Pre- Grouting Test #2 and Pre-Grouting Test #1 .....	87
Figure 2.11 2-D and 3-D Tomographic Interpretation of the Geometry and Location of the Defect at A2-4 .....	88
Figure 2.12 Location of the Coreholes and CSL Tubes of the A2-4 .....	90
Figure 2.13 Coring Procedure of the A2-4 at Site # 2 Bridge .....	90
Figure 2.14 (a-c) Cores from the SE Core Hole (in Between CSL Tubes 2-3) and (d-g) Cores from the Corehole in-between CSL Tubes 1-3 of the A2-4 Drilled Shaft for “Site 2 Bridge.....	92
Figure 2.15 Close-Up Look at the Defect with Velocity Reduction Counters (30% & 50% Reduction) .....	93
Figure 2.16 Close-Up Look at the Defect with Velocity Reduction Counters (20% Reduction and Combination of all).....	94
Figure 2.17 (a) & (b) Mechanism Used for Pressure Grouting .....	96
Figure 2.18 Difference Tomograms in Between Post-Grouting Test and Pre-Grouting Test #2 .....	97
Figure 2.19 CSL Retest Results After Pressure Grouting.....	98
Figure 3.1 Temperature Monitoring of A1-S1 at 6 hrs. (Black), 12 hrs. (Blue) and 24 hrs. (Red) after Concrete Placement .....	103

Figure 3.2 Temperature Monitoring of A1-S1 at 6 hrs. (Black), 12 hrs. (Blue), 24 hrs. (Red), 2 days (Green), 3 days (Purple), 4 days (Orange), 5 days (Teal), and 6 days (Yellow) after Concrete Placement .....	104
Figure 3.3 Temperature Monitoring of A1-S1 Averaged from the 4 Access Tubes at Depths of 3m (Black), 6 m (Blue), 9 m (Red), 12 m (Green), and 15 m (Magenta).....	105
Figure 3.4 Temperature Monitoring of P2-S2. Temperatures at 1 hr. (Black), 24 hrs. (Red), 2 days (Green), 3 days (Purple), 4days (Orange), 5 days (Teal) and 6 days (Yellow) after Concrete Placement .....	107
Figure 3.5 Temperature Monitoring of P2-S2. Temperatures are Averaged from the 4 Access Tubes at depths of 0.8 m (Black, Gravel), 5 m (Blue, Clay), 10 m (Red, Clay), and 12.5 m (Green, Shale Bedrock) .....	108
Figure 3.6 Temperatures from Embedded Thermocouples of A2-S2- Red at the Center of Shaft at 2.4 m, Blue Near Rebar Cage at Same Depth, and Green Temperature Differential Between Both Stations.....	110
Figure 3.7 Temperatures from Embedded Thermocouples of Shaft P-3 at Site 2 Near Rebar Cage- Red at 3.66 m (Above Groundwater Table), Blue at 12.8 m (Below Groundwater Table), and Green is Temperature Differential Between Both Stations .....	111
Figure 3.8 CSL Velocity Measurements of A1-S1- Velocities at 1 day (Red), 2 days (Green), 3 days (Purple), 4 days (Orange), 5 days (Teal), and 6days (Yellow) After Concrete Placement.....	114
Figure 3.9 CSL Velocity Measurements of A1-S1 between Tubes 1-3 and 2-4 at 1 day (Red), 2days (Green), 3 days (Purple), 4 days (Orange), 5 days (Teal), and 6 days (Yellow) after Concrete Placement .....	116
Figure 3.10 Average CSL Velocity Measurements of A1 S1. Static Corrected Velocity Values are Averaged from the 4 Access Tubes (and Six CSL Test Paths) at Depths of 3m (Black), 6 m (Blue), 9 m (Red), 12 m (Green), and 15 m (Magenta).....	117
Figure 3.11 CSL Velocity Measurements of P2- S2- at 3 days (Purple) and 4 days (Orange) After Concrete Placement.....	118
Figure 3.12 CSL Velocity Measurements of P2- S2- between Tubes 1-3 and 2-4 at 3 days (Purple) and 4 days (Orange) After Concrete Placement .....	119
Figure 3.13 GDL Density Monitoring of A1-S1- with 1 day (Red), 2 days (Green), 3 days (Purple),and 4 days (Orange) After Concrete Placement .....	120

Figure 3.14 Average GDL Density Monitoring of A1-S1- Densities are Averaged from the 4 Access Tubes at Depths of 3 m (Black), 6 m (Blue), 9 m (Red), 12 m (Green), and 15 m (Magenta) .....	121
Figure 3.15 GDL Density Monitoring of P2-S2. Densities at 1 day (Red), 2 days (Green), 3 days (Purple), and 4 days (Orange) After Concrete Placement..	122
Figure 3.16 NML Moisture Monitoring of A1-S1- at 1 day (Red), 2 days (Green), 3 days (Purple), 4 days (Orange), 5 days (Teal), and 6 days (Yellow) After Concrete Placement .....	124
Figure 3.17 NML Moisture Monitoring of A1-S1. Moisture Values are Averaged from the 4 Access Tubes at Depths of 3 m (Black), 6 m (Blue), 9 m (Red), 12 m (Green), and 15 m (Magenta) .....	126
Figure 3.18 NML Moisture Monitoring of P2-S2- at 2 days (Green), 3 days (Purple), and 4 days (Orange) After Concrete Placement .....	127
Figure 4.1 Typical Rate of Heat Evolution during Cement Hydration.....	132
Figure 4.2 Temperature Plot from Data Progressively Collected from Access Tubes .....	142
Figure 5.1 2D and 3D Thermal Network Mesh for Heat Conducting Calculations	159
Figure 5.2 Visco-Elastic Contact Model for DEM .....	167
Figure 5.3 Blocks in Contact .....	169
Figure 5.4 Identical Elastic Rough Spheres in Contact .....	174
Figure 5.5 Hertz Contact of Solids of Revolution .....	175
Figure 5.6 Stack Balls Setup for Energy and Dynamic Relaxation Numerical Tests .....	180
Figure 5.7 Total Energy of Stack Ball .....	181
Figure 5.8 Dynamic Relaxation Test Results .....	183
Figure 5.9 1-D P-Wave Propagation in a Rod .....	185
Figure 6.1 Material Palettes used in GAP Models. Defects Shown in Red Include Honeycombs, Cracking, and Debonding. Darker Colors on the Left Represent Lower Values. These Palettes are used to Display Corresponding Velocity, Wave Compression, Average Stress, Temperature, Heat Generation, Hydration Phase, Tension Strength, Modulus, etc. A Cross-section of the 1 m Drilled Shaft used in the Study is Shown on the Right. The Shaft is in the Center, Surrounded by Dry Sand, Wet Sand, Clay, and Rock. Portions of the	

Wet Sand, Clay, and Concrete are Hidden to Show the Internals of the Model.	187
Figure 6.2 Location of Drilled Shaft Cross-section Surrounded by Rock	191
Figure 6.3 Location of 3D Section within Drilled Shaft	192
Figure 6.4 Rock (Top Left) vs. Clay (Top Right) at 20 $\mu$ s, with Difference (Bottom)	196
Figure 6.5 Rock (Top Left) vs. Clay (Top Right) at 60 $\mu$ s, with Difference (Bottom)	197
Figure 6.6 Rock (Top Left) vs. Clay (Top Right) at 120 $\mu$ s, with Difference (Bottom)	198
Figure 6.7 Rock (Top Left) vs. Clay (Top Right) at 300 $\mu$ s, with Difference (Bottom)	199
Figure 6.8 Rock (Top Left) vs. Clay (Top Right) at 500 $\mu$ s, with Difference (Bottom)	200
Figure 6.9 CSL Signals from Rock vs. Clay, between Access Tubes 1 and 2 (Top), and Tubes 1 and 3 (Bottom)	201
Figure 6.10 No Rebar (Top Left) vs. Rebar (Top Right) at 20 $\mu$ s, with Difference (Bottom)	206
Figure 6.11 No Rebar (Top Left) vs. Rebar (Top Right) at 20 $\mu$ s, with Difference (Bottom)	207
Figure 6.12 No Rebar (Top Left) vs. Rebar (Top Right) at 120 $\mu$ s, with Difference (Bottom)	208
Figure 6.13 No Rebar (Top Left) vs. Rebar (Top Right) at 300 $\mu$ s, with Difference (Bottom)	209
Figure 6.14 No Rebar (Top Left) vs. Rebar (Top Right) at 500 $\mu$ s, with Difference (Bottom)	210
Figure 6.15 CSL Signals from No Rebar vs. Rebar, between Access Tubes 1 and 2 (Top), and Tubes 1 and 3 (Bottom)	211
Figure 6.16 PVC (Top Left) vs. Steel (Top Right) Access Tubes at 20 $\mu$ s, with Difference (Bottom)	215
Figure 6.17 PVC (Top Left) vs. Steel (Top Right) Access Tubes at 20 $\mu$ s, with Difference (Bottom)	216

Figure 6.18 PVC (Top Left) vs. Steel (Top Right) Access Tubes at 120 $\mu$ s, with Difference (Bottom).....	217
Figure 6.19 PVC (Top Left) vs. Steel (Top Right) Access Tubes at 300 $\mu$ s, with Difference (Bottom).....	218
Figure 6.20 PVC (Top Left) vs. Steel (Top Right) Access Tubes at 500 $\mu$ s, with Difference (Bottom).....	219
Figure 6.21 CSL Signals from PVC vs. Steel Access Tubes, between Tubes 1 and 2 (Top), and Tubes 1 and 3 (Bottom) .....	220
Figure 6.22 Tube Debonding (Top Left) vs. No Tube Debonding (Top Right) at 20 $\mu$ s, with Difference (Bottom).....	225
Figure 6.23 Debonding (Top Left) vs. No Tube Debonding (Top Right) at 20 $\mu$ s, with Difference (Bottom).....	226
Figure 6.24 Debonding (Top Left) vs. No Tube Debonding (Top Right) at 120 $\mu$ s, with Difference (Bottom).....	227
Figure 6.25 Debonding (Top Left) vs. No Tube Debonding (Top Right) at 300 $\mu$ s, with Difference (Bottom).....	228
Figure 6.26 Debonding (Top Left) vs. No Tube Debonding (Top Right) at 500 $\mu$ s, with Difference (Bottom).....	229
Figure 6.27 CSL Signals with Tube Debonding vs. No Tube Debonding, between Access Tubes 1 and 2 (Top), and Tubes 1 and 3 (Bottom).....	230
Figure 6.28 Outside Sensor Drift (Top Left) vs. Inside Sensor Drift (Top Right) at 20 $\mu$ s, with Difference (Bottom).....	232
Figure 6.29 Outside Sensor Drift (Top Left) vs. Inside Sensor Drift (Top Right) at 20 $\mu$ s, with Difference (Bottom).....	233
Figure 6.30 Outside Sensor Drift (Top Left) vs. Inside Sensor Drift (Top Right) at 120 $\mu$ s, with Difference (Bottom).....	234
Figure 6.31 Outside Sensor Drift (Top Left) vs. Inside Sensor Drift (Top Right) at 300 $\mu$ s, with Difference (Bottom).....	235
Figure 6.32 Outside Sensor Drift (Top Left) vs. Inside Sensor Drift (Top Right) at 500 $\mu$ s, with Difference (Bottom).....	236
Figure 6.33 CSL Signals with Outside Sensor Drift vs. Inside Sensor Drift, between Access Tubes 1 and 2 (Top), and Tubes 1 and 3 (Bottom).....	237

Figure 6.34 Cracking Defect (Top Left) vs. No Defect (Top Right) at 20 $\mu$ s, with Difference (Bottom).....	240
Figure 6.35 Cracking Defect (Top Left) vs. No Defect (Top Right) at 20 $\mu$ s, with Difference (Bottom).....	241
Figure 6.36 Cracking Defect (Top Left) vs. No Defect (Top Right) at 120 $\mu$ s, with Difference (Bottom).....	242
Figure 6.37 Cracking Defect (Top Left) vs. No Defect (Top Right) at 300 $\mu$ s, with Difference (Bottom).....	243
Figure 6.38 Cracking Defect (Top Left) vs. No Defect (Top Right) at 500 $\mu$ s, with Difference (Bottom).....	244
Figure 6.39 CSL Signals with a Cracking Defect vs. No Defect, between Access Tubes 1 and 2 (Top), and Tubes 1 and 3 (Bottom).....	245
Figure 6.40 Honeycomb Defect (Top Left) vs. No Defect (Top Right) at 20 $\mu$ s, with Difference (Bottom).....	249
Figure 6.41 Honeycomb Defect (Top Left) vs. No Defect (Top Right) at 20 $\mu$ s, with Difference (Bottom).....	250
Figure 6.42 Honeycomb Defect (Top Left) vs. No Defect (Top Right) at 120 $\mu$ s, with Difference (Bottom).....	251
Figure 6.43 Honeycomb Defect (Top Left) vs. No Defect (Top Right) at 300 $\mu$ s, with Difference (Bottom).....	252
Figure 6.44 Honeycomb Defect (Top Left) vs. No Defect (Top Right) at 500 $\mu$ s, with Difference (Bottom).....	253
Figure 6.45 CSL Signals with a Honeycomb Defect vs. No Defect, between Access Tubes 1 and 2 (Top), and Tubes 1 and 3 (Bottom).....	254
Figure 6.46 Void Defect (Top Left) vs. No Defect (Top Right) at 20 $\mu$ s, with Difference (Bottom).....	257
Figure 6.47 Void Defect (Top Left) vs. No Defect (Top Right) at 20 $\mu$ s, with Difference (Bottom).....	258
Figure 6.48 Void Defect (Top Left) vs. No Defect (Top Right) at 120 $\mu$ s, with Difference (Bottom).....	259
Figure 6.49 Void Defect (Top Left) vs. No Defect (Top Right) at 300 $\mu$ s, with Difference (Bottom).....	260

Figure 6.50 Void Defect (Top Left) vs. No Defect (Top Right) at 500 $\mu$ s, with Difference (Bottom).....	261
Figure 6.51 CSL Signals with a Void vs. No Defect, between Access Tubes 1 and 2 (Top), and Tubes 1 and 3 (Bottom) .....	262
Figure 7.1 Rate of Heat Generation (Cal/hr) used in the Numerical Model.....	264
Figure 7.2 Curing Compression. Top: 4 hours. Bottom: 8 hours. Left: Rock. Middle: Clay. Right: Difference .....	270
Figure 7.3 Curing Compression. Top: 12 hours. Bottom: 24 hours. Left: Rock. Middle: Clay. Right: Difference .....	272
Figure 7.4 Curing Compression. Top: 2 days. Bottom: 3 days. Left: Rock. Middle: Clay. Right: Difference .....	274
Figure 7.5 Curing Compression. Top: 4 days. Bottom: 5 days. Left: Rock. Middle: Clay. Right: Difference .....	275
Figure 7.6 Curing Fracture. Top: 4 hours. Bottom: 8 hours. Left: Rock. Middle: Clay. Right: Difference .....	277
Figure 7.7 Curing Fracture. Top: 12 hours. Bottom: 24 hours. Left: Rock. Middle: Clay. Right: Difference .....	279
Figure 7.8 Curing Fracture. Top: 2 days. Bottom: 3 days. Left: Rock. Middle: Clay. Right: Difference .....	280
Figure 7.9 Curing Fracture. Top: 4 days. Bottom: 5 days. Left: Rock. Middle: Clay. Right: Difference .....	281
Figure 7.10 Curing Heat. Top: 4 hours. Bottom: 8 hours. Left: Rock. Middle: Clay. Right: Difference .....	283
Figure 7.11 Curing Heat. Top: 12 hours. Bottom: 24 hours. Left: Rock. Middle: Clay. Right: Difference .....	284
Figure 7.12 Curing Heat. Top: 2 days. Bottom: 3 days. Left: Rock. Middle: Clay. Right: Difference .....	285
Figure 7.13 Curing Heat. Top: 4 days. Bottom: 5 days. Left: Rock. Middle: Clay. Right: Difference .....	287
Figure 7.14 Curing Hydration. Top: 4 hours. Bottom: 8 hours. Left: Rock. Middle: Clay. Right: Difference .....	288
Figure 7.15 Curing Hydration. Top: 12 hours. Bottom: 24 hours. Left: Rock. Middle: Clay. Right: Difference .....	289

Figure 7.16 Curing Hydration. Top: 2 days. Bottom: 3 days. Left: Rock. Middle: Clay. Right: Difference .....	290
Figure 7.17 Curing Hydration. Top: 4 days. Bottom: 5 days. Left: Rock. Middle: Clay. Right: Difference .....	291
Figure 7.18 Curing Temperature. Top: 4 hours. Bottom: 8 hours. Left: Rock. Middle: Clay. Right: Difference .....	292
Figure 7.19 Curing Temperature. Top: 12 hours. Bottom: 24 hours. Left: Rock. Middle: Clay. Right: Difference .....	294
Figure 7.20 Curing Temperature. Top: 2 days. Bottom: 3 days. Left: Rock. Middle: Clay. Right: Difference .....	295
Figure 7.21 Curing Temperature. Top: 4 days. Bottom: 5 days. Left: Rock. Middle: Clay. Right: Difference .....	297
Figure 8.1 Compression Stress at Initial Vertical Displacement. Top: Sand Intrusion at 1 m Depth. Bottom: Sand Intrusion 3 m Depth. Left: Compression Stress, No Defect. Center: Compression Stress. Right: Compression Stress Difference .....	302
Figure 8.2 Fracture Extent at Initial Vertical Displacement. Top: Sand Intrusion at 1 m Depth. Bottom: Sand Intrusion 3 m Depth. Left: Fractures, No Defect. Center: Fractures. Right: Fracture Difference .....	303
Figure 8.3 Compression Stress at 4 cm Vertical Displacement. Top: Sand Intrusion at 1 m Depth. Bottom: Sand Intrusion 3 m Depth. Left: Compression Stress, No Defect. Center: Compression Stress. Right: Compression Stress Difference .....	305
Figure 8.4 Fracture Extent at 4 cm Vertical Displacement. Top: Sand Intrusion at 1 m Depth. Bottom: Sand Intrusion 3 m Depth. Left: Fractures, No Defect. Center: Fractures. Right: Fracture Difference .....	306
Figure 8.5 Compression Stress at 8 cm Vertical Displacement. Top: Sand Intrusion at 1 m Depth. Bottom: Sand Intrusion 3 m Depth. Left: Compression Stress, No Defect. Center: Compression Stress. Right: Compression Stress Difference .....	308
Figure 8.6 Fracture Extent at 8 cm Vertical Displacement. Top: Sand Intrusion at 1 m Depth. Bottom: Sand Intrusion 3 m Depth. Left: Fractures, No Defect. Center: Fractures. Right: Fracture Difference .....	309
Figure 8.7 Compression Stress at 12 cm Vertical Displacement. Top: Sand Intrusion at 1 m Depth. Bottom: Sand Intrusion 3 m Depth. Left: Compression Stress,	

No Defect. Center: Compression Stress. Right: Compression Stress Difference .....	311
Figure 8.8 Fracture Extent at 12 cm Vertical Displacement. Top: Sand Intrusion at 1 m Depth. Bottom: Sand Intrusion 3 m Depth. Left: Fractures, No Defect. Center: Fractures. Right: Fracture Difference .....	312
Figure 8.9 Compression Stress at 16 cm Vertical Displacement. Top: Sand Intrusion at 1 m Depth. Bottom: Sand Intrusion 3 m Depth. Left: Compression Stress, No Defect. Center: Compression Stress. Right: Compression Stress Difference .....	314
Figure 8.10 Fracture Extent at 16 cm Vertical Displacement. Top: Sand Intrusion at 1 m Depth. Bottom: Sand Intrusion 3 m Depth. Left: Fractures, No Defect. Center: Fractures. Right: Fracture Difference .....	315
Figure 8.11 Compression Stress at 20 cm Vertical Displacement. Top: Sand Intrusion at 1 m Depth. Bottom: Sand Intrusion 3 m Depth. Left: Compression Stress, No Defect. Center: Compression Stress. Right: Compression Stress Difference .....	316
Figure 8.12 Fracture Extent at 20 cm Vertical Displacement. Top: Sand Intrusion at 1 m Depth. Bottom: Sand Intrusion 3 m Depth. Left: Fractures, No Defect. Center: Fractures. Right: Fracture Difference .....	317
Figure 8.13 Effect of a Defect at Two Different Depths on Load Bearing Capacity .....	319
Figure 8.14 Effect of a Defect on Load Bearing Capacity with Shaft in Compacted Soil .....	321
Figure 8.15 Effect of Soil Compaction on Load Bearing Capacity .....	322

## TABLES

Table 1.1 Numerical Relationship between Path Length (PL), Transit Time (TT), Frequency (f), Period ( $T=1/f$ ), Velocity ( $V=PL/TT$ ), and Wavelength ( $\lambda=V/f$ ) .....	42
Table 1.2 Recommended Number of Access Tubes Versus Shaft Diameter (Olson Engineering, Inc.).....	45
Table 1.3 Technical Specification for the PILELOG - CSL system.....	51
Table 1.4 Transducers Specifications .....	53
Table 2.1 CSL Results from the Eight Shafts at Abutments 1 and 2, Site 1.....	72
Table 2.2 Summary of CSL Results at Site 2 .....	80
Table 4.1 Properties of Typical Ceramics.....	129
Table 4.2 Compounds Involved in the Concrete Curing Process (Kosmatka 2002) .....	131
Table 4.3 Surface Cracking Risks for a Structure with Concrete Thickness of 1.5 m .....	139
Table 4.4 Effects on Crack Sensitivity (Springenschmid 1998).....	144
Table 4.5 Comparison of Measures on $\Delta T$ , Concrete Strength, and Overall Concrete Quality.....	147
Table 4.6 Ground Water Flow in Soil.....	151
Table 6.1 Property Ranges Corresponding to Material Color Palettes.....	188
Table 6.2 Material Properties used in Models .....	189
Table 6.3 Thermal Expansion of PVC and Steel (inches/100 ft).....	221
Table 7.1 Curing Model Coefficients .....	265